ChemComm
Chemical Communications

Accepted Manuscript

This article can be cited before page numbers have been issued, to do this please use: T. li, F. Huo, J. Chao and C. Yin, *Chem. Commun.*, 2020, DOI: 10.1039/D0CC04839A.

ROYAL SOCIETY OF CHEMISTRY

rsc.li/chemcomm

View Article Online
DOI: 10.1039/D0CC04839A

COMMUNICATION

Independent bi-reversible reactions and regulable FERT efficiency achieving Cys metabolism SO_2 real-time process visualization

Received 00th January 20xx,
Accepted 00th January 20xx

DOI: 10.1039/x0xx00000x

Tao Li, [a] Fangjun Huo,[b] Jianbin Chao,[b] and Caixia Yin*[a]

In this work, we synthesized an independent bi-reversible reactions sensor BPC for simultaneously detecting cysteine (Cys) and sulfur dioxide (SO_2), showing multi-fluorescent signal modes due to the regulable FRET efficiency, and finally achieving real-time process visualization of Cys metabolism SO_2 in subcellular organelle and tumor.

Metabolism refers to the pathway in which organisms achieve self-renewal by dynamically exchanging substances and energy with the external environment. However, as one of them, the biochemical process of substance metabolism of cysteine (Cys) in *vivo* has not been well cognized. As a nature amino acid containing reducing mercapto (-SH) group, Cys is directly involved in many crucial life processes such as nutritional intake, antioxidant, protein synthesis, metabolism.[1] The concentration unbalance of Cys in organisms is closely associated with Parkinson's disease, Alzheimer's disease and liver injury.[2] Cys mainly is generated in mammalian cells through three biotransformation pathways: (a) methionine metabolism, (b) proteolysis, (c) cystine reduction [note that Cys exists mainly in the state of disulfide bonds in the blood system due to the high oxidation environment in plasma].[3] In aerobic condition, Cys will be catalyzed to form cysteine sulfinate by cysteine dioxygenase (CDO), and then enzymatically converted to *β*-sulfinylpyruvate by aspartate aminotransferase (AAT), eventually spontaneously decomposed to pyruvate and sulfur dioxide (SO_2), which is excreted in the urine in the form of its derivatives (SO_3^{2-} / HSO_3^-).[4] Interestingly, it has be reported that endogenous SO_2 can regulate vascular smooth muscle tone and act as an antioxidant to protect the redox balance in cells, thereby improving cardiovascular function.[5] Additionally, targeting mitochondria, where Cys and SO_2 are mainly produced and stored in eukaryotic cells, will provide a deeper perspective to perceive the complex physiological interrelationship between them.[6] Thus, given the above-mentioned physiological and pathological effects of Cys and its metabolite SO_2, a simple, effective and reliable strategy is urgently needed to probe concentration fluctuation and track its metabolic pathways in cells and organisms, which is of great significance in preventing related diseases.

To date, as these outstanding features including simple operation, noninvasiveness and real-time visualization, fluorescent probes with molecular imagine technology have become an ideal platform for exploring the distribution of small biomolecules in living organisms and their corresponding biological effects.[7] In the past decade, great progress has been made in efforts to develop detection of Cys or SO_2 using fluorescent probe,[8] but only a few breakthroughs have been acquired in evaluating their metabolic relationships. For example, in 2017, our group firstly reported a turn-on fluorescent probe with dual-site to visualize the metabolism of Cys in living cells.[3a] In 2018, Zhang et al. developed a ratiometric fluorescent probe to explore the kinetic process of SO_2 in hepatic BRL cells after treating excess exogenous Cys.[8c] However, the defects specific to these probes: (a) the inability to monitor the simultaneous presence of Cys and its metabolite SO_2, (b) long time to detect the analytes, and (c) insufficient sensitivity to meet the detection requirements of SO_2 as a low concentration of transient metabolite. These mean that the microscopic physiological process of Cys metabolism cannot be truly understood and visualized. Inspired by the above probes and the characteristics of Cys metabolism, we further came up with a perception: the ideal probe needs to meet independent bi-reversible reaction sites and fast response toward analytes.

To satisfy the above-mentioned demands, we proposed a strategy to achieving simultaneously detection of Cys and SO_2 by employing the FRET mechanism. To make it a reality, the coumarin moiety of **CP** was selected as the energy donor and the *α, β*-unsaturated C=C double bond as the recognition site

[a] *Key Laboratory of Chemical Biology and Molecular Engineering of Ministry of Education, Key Laboratory of Materials for Energy Conversion and Storage of Shanxi Province, Institute of Molecular Science, Shanxi University, Taiyuan 030006, China. E-mail: yincx@sxu.edu.cn*
[b] *Research Institute of Applied Chemistry, Shanxi University, Taiyuan 030006, China.*
Electronic Supplementary Information (ESI) available: [details of any supplementary information available should be included here]. See DOI: 10.1039/x0xx00000x

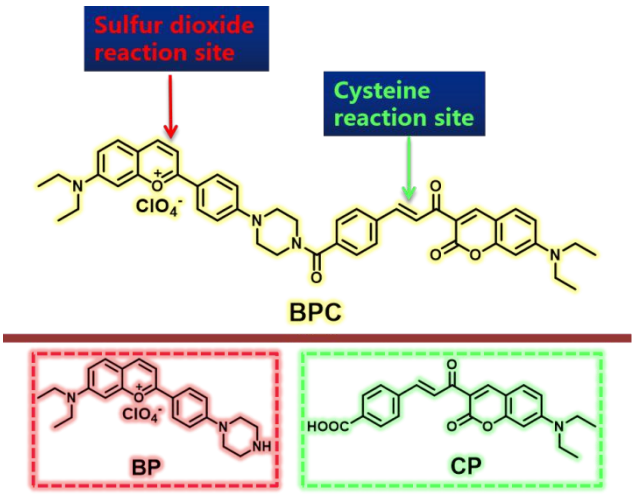

Scheme 1. Design of sensor **BPC.**

toward Cys (Fig. S5a), which could recover its original state by introducing a thiol scavenger, N-ethylmaleimide (NEM).[9] Meanwhile, it was found that the **BP** showed high sensitivity for SO_2 (Fig. S5b), which was reversible due to the interaction with formaldehyde (HCHO).[10] Coincidentally, the fluorescent emission wavelength of **CP**-**Cys** has a lot of overlap with the absorbance of **BP**, which can ensure the FRET effect of the probe internal (Fig. S5c). In this work, we combined **BP** with **CP** to create an independent bi-reversible reactions sensor **BPC** for dynamically tracking SO_2 metabolism from Cys (Scheme 1). As shown in Scheme S2, Cys can attack the *α, β*-unsaturated C=C double bond by the nucleophilic addition reaction, resulting in the red fluorescent signal distinctly enhancement due to the FRET process from the energy donor **CP**-**Cys** to the acceptor **BP**. Subsequently, adding the SO_2 to the mixture of **BPC-Cys**, the π-conjugated system of benzopyrylium unit was interrupted, causing the red fluorescent signal to decrease due to the disappearance of the energy acceptor **BP** and releasing the fluorescent emission of the energy donor **CP**-**Cys.** Therefore, **BPC** can achieve the simultaneously detection of Cys and SO_2 through independent bi-reversible reactions and luminescence regulated by FRET strategy.

To verify our conception, we firstly recorded the fluorescent spectra of **BPC** (10 μM) toward Cys. As exhibited in Fig. 1a, the fluorescence intensity at 500 nm and 637 nm both gradually increased (excitation wavelength at 430 nm) along with the addition of Cys (0-40 equiv.), which was due to the nucleophilic addition reaction caused by Cys to form the energy donor **CP-Cys** and the special efficiency of the FRET mechanism was calculated to be 51.2 % ($E = 1 - F_{DA}/F_D$, Fig. S5d).[11] The detection limit was 2.9 μM based on IUPAC (CDL = $3S_b/m$),[12] and the equilibrium was obtained after 4 min with adding different concentrations of Cys (Fig. S1a, b). Interestingly, we found that the emission peak at 637 nm was rapidly quenched when Na_2SO_3 at low concentrations (0-4 equiv.) was added to **BPC** (Fig. 1b, excitation wavelength at 585 nm), and under the excitation wavelength at 430 nm, the fluorescent signal at 500 nm had slight increase (Fig. S2c) showing that the π-conjugated system of benzopyrylium unit

View Article Online
DOI: 10.1039/D0CC04839A

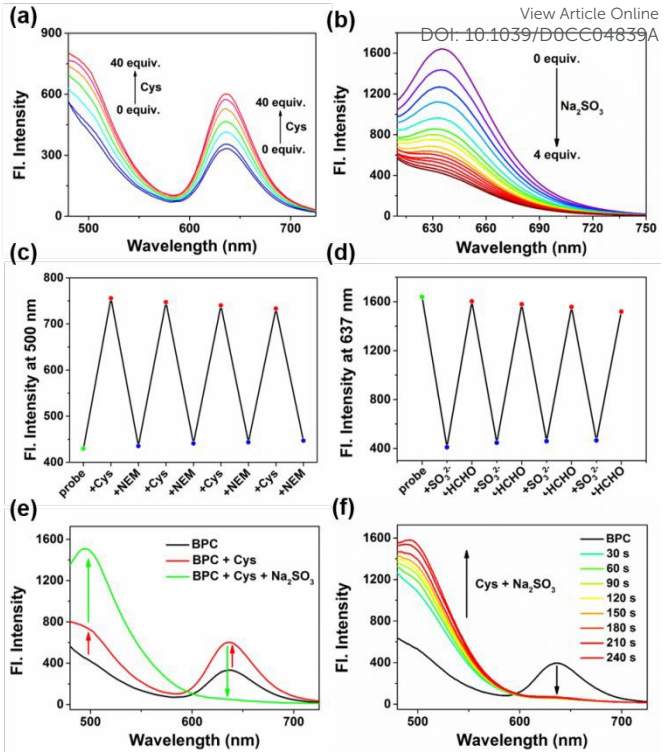

Fig. 1 (a) or (b) The fluorescent spectra of probe **BPC** (10 μM) toward Cys (0-40 equiv.) or Na_2SO_3 (0-4 equiv.), λ_{ex} = 430 nm, λ_{em} = 500 nm; and λ_{ex} = 585 nm, λ_{em} = 637 nm, slit: 5 nm/10 nm. (c) The reversible cycle of probe **BPC** (10 μM) with Cys (40 equiv.) upon addition of NEM (40 equiv.), λ_{ex} = 430 nm, λ_{em} = 500 nm, slit: 5 nm/10 nm. (d) The fluorescent change of probe **BPC** (10 μM) upon the addition of Na_2SO_3 (4 equiv.) or HCHO (4 equiv.) consecutively, λ_{ex} = 585 nm, λ_{em} = 637 nm, slit: 5 nm/10 nm. Condition: DMSO/PBS solution (10.0 mM, pH = 7.4, 1:9, v/v). (e) or (f) The fluorescence spectra of **BPC** (10 μM) upon the treatment of Cys (40 equiv.) and Na_2SO_3 (4 equiv.) in turn or simultaneously, λ_{ex} = 430 nm, λ_{em} = 500 nm and λ_{em} = 637 nm, slit: 5 nm/10 nm. Condition: DMSO/PBS solution (10.0 mM, pH = 7.4, 1:9, v/v).

was interrupted (Fig. S2d). Under this condition, the special efficiency of the FRET mechanism was 14.5 % ($E = 1 - F_{DA}/F_D$, Fig. S2e).[11] Owing to the quick detection time (20 s) and low detection limit 0.14 μM, it can perfectly meet the detection requirements of SO_2 as a transient metabolite of Cys in cells (Fig. S2a, b).

We then confirmed the reversibility of **BPC** toward Cys or SO_2, respectively. Fortunately, upon addition of NEM in the presence of Cys, the fluorescent emission peak of **BPC-Cys** at 500 could be decreased to its original state and recovered by introducing Cys into the solution again (Fig. 1c), which was consistent with our idea that NEM can capture Cys from the compound **BPC**-**Cys** to release free **BPC**. According to the previous literature reported, HCHO as an electrophile can effectively react with SO_2.[10] After adding the HCHO, the fluorescent intensity of **BPC**-$\mathbf{SO_2}$ at 637 nm gradually increased to near the initial level of **BPC** and further quenched by adding equivalent Na_2SO_3 (Fig 1d). Consequently, the probe **BPC** can be considered as an

View Article Online
DOI: 10.1039/D0CC04839A

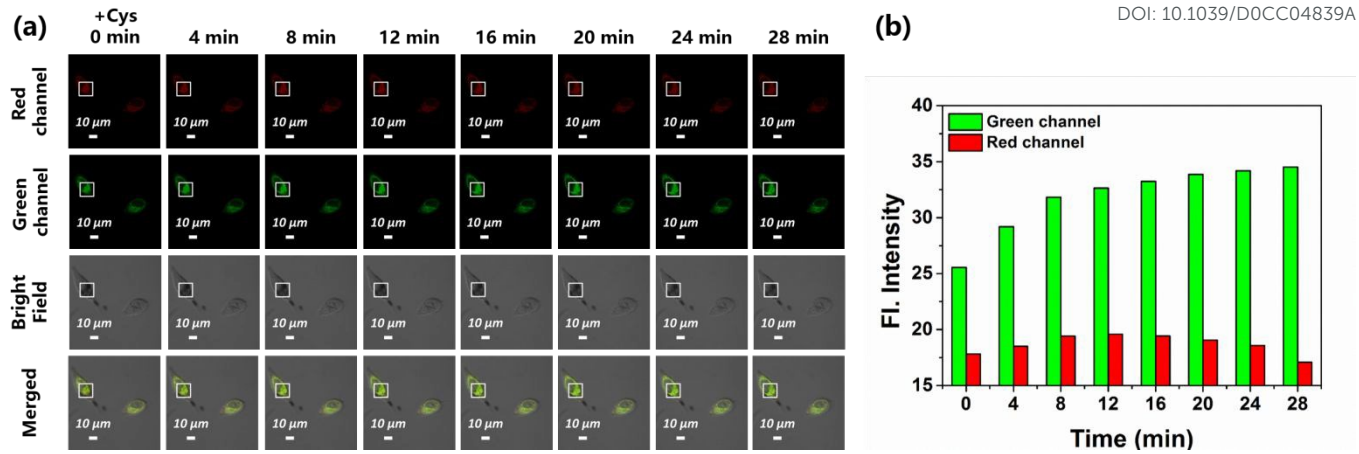

Fig. 2 Real-time visualizing Cys metabolism in cells using **BPC**: (a) the time-dependented images of **BPC** (10 μM) incubated HeLa cells after adding Cys (400 μM) every 4 min (from 0 to 28 min); (b) Corresponding average fluorescence intensities of red and green channel in every 4 min (from 0 to 28 min). Red channel, λ_{em} = 610-670 nm and Green channel, λ_{em} = 470-530 nm, λ_{ex} = 458 nm. Scale bar: 10 μm.

ideal candidate to achieve the reversible detection of Cys or SO_2, individually.

Inspired by the above data, we wondered if **BPC** could be applied more profoundly to investigate Cys-SO_2 metabolism. As described in Fig. 1e, the fluorescence peaks of **BPC** at 500 nm and 637 nm initially enhanced after the treatment with Cys due to this special FRET mechanism. Subsequently, upon the addition of Na_2SO_3 to the mixture of **BPC-Cys**, the fluorescence peak at 637 nm disappeared promptly while a sharp increase at 500 nm simultaneously, which was due to the disappearance of the energy acceptor **BP** and the release of the fluorescence of the energy donor **CP-Cys.** The 137 nm fluorescent blue-shift indicated the disruption of the FRET strategy from **CP-Cys** to **BP** and the formation of reaction product (**BPC-Cys-SO_2**). Because Cys and SO_2 coexist in complicated physiological system, we added them synchronously. As explicated in Fig. 1f, this situation was consistent with the above consequence, just consuming 4 min to reach equilibrium, meaning that **BPC** can take on the task of simultaneously detecting Cys and SO_2.

The sensing mechanism of **BPC** for detecting Cys and SO_2 was described in Scheme S2. The corresponding reaction products were proved by ESI-MS characterization. The highest peak at *m/z* 735.35436 represented **BPC** in Fig. S6. Obviously, there was a main peak at *m/z* 856.37438 corresponding to the **BPC-Cys** product (Fig. S7). As described in Fig. S8, it can be ascribed the dominant peak at *m/z* 815.31147 to the deserved mixture of **BPC-SO_2**. The final product **BPC-Cys-SO_2** was *m/z* 936.33250 (Fig. S9). These conclusive evidences signified that the principles for **BPC** responding Cys or SO_2 all conformed with our previous conception.

Therefore, the above series of in vitro spectral response results demonstrated that the probe **BPC** may have potential to become an effective and reliable tool in tracking Cys metabolic pathways in cells and organisms. Then we conducted biological imaging experiments to evaluate the feasibility of this conjecture. We initially explored the cytotoxicity of **BPC** by MTT assay (Fig. S10). It should be noted that HeLa cells incubated with **BPC** (0-10 μM) for 12 h still show high survival rates. Since **BPC** with a positively charged part, we guessed that it could locate the mitochondria. As shown in Fig. S11, HeLa cells were sequentially incubated with **BPC** (10 μM) and MitoTracker Green (0.2 μM). The fluorescent signal of red and green channels shown synchronous tendency and the Pearson's co-localization coefficient of 0.88, which well revealed the **BPC** can serve as the mitochondrial targeting tool.

We next conducted the fluorescent imaging of exogenous SO_2 (Na_2SO_3). To demonstrate that **BPC** can still function as FRET in cellular level, we used a single wavelength to excite different channels. After HeLa cells treated with 10 μM **BPC** for 20 min, then removed the residue, adding the Na_2SO_3 (40 μM) the red fluorescence signal gradually declined from 0 to 12 min (Fig. S12). To confirm the above-mentioned reversibility, adding HCHO (40 μM) into above system, the fluorescent intensity in red channel gradually increased with time. This phenomenon suggested that **BPC** can in *situ* real-time reversible imaging of exogenous SO_2 in living cells. Related literature reported that high level of Cys can stimulate CDO activity,[13] then SO_2 was metabolized. Subsequently, we tried to real-time visualize Cys metabolism in cells using **BPC**. HeLa cells were incubated with **BPC** (10 μM) in turn and Cys (400 μM) for imaging. As is described in Fig. 2, the time-dependent imaging showed a gradual increase of fluorescence signals in the red and green channels from 0 to 12 min, indicating that Cys entered the cells and reacted with **BPC**. Then, the red fluorescence suddenly decreased while the green fluorescence kept rising, meaning the endogenous SO_2 also generated and be detected. From the above phenomena, **BPC** possesses multi-fluorescence modes to investigate and visualize the process for SO_2 metabolism from Cys in mitochondria of living cells.

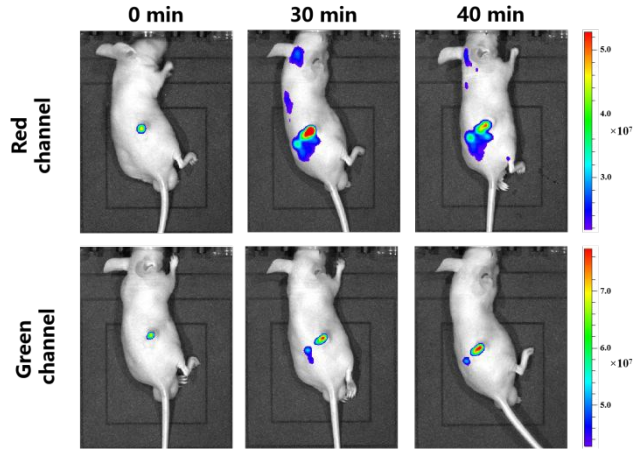

Fig. 3 The metabolic imaging of Cys (400 μM) using **BPC** in HeLa tumor-bearing nude mice at different time, Red channel: λ_{em} = 610-670 nm; and Green channel: λ_{em} =470-530 nm, λ_{ex} = 430 nm.

To further explore the application in biological aspects, we established a mouse tumor biological model for visualizing the Cys metabolism. The tumor areas in mice with HeLa cells, as described in Fig. 3, displayed the weak red and green fluorescent signals after injection **BPC** (20 μM). When exogenous Cys (400 μM) was added to this tumor areas, the fluorescence signal in red channel reached the maximum after 30 min, followed by declined over time. This phenomenon may be due to the high level of SO_2 produced through by the enzymaticly metabolic reaction of Cys in tumor areas, resulting in red fluorescence decreased.

In summary, we firstly synthesized an independent bi-reversible reactions sensor **BPC** for precisely dynamic real-time process visualization of Cys metabolism SO_2. Based on the special FRET mechanism, **BPC** can emit completely different fluorescent signal patterns with increased or decreased red fluorescence corresponding to Cys and SO_2. Furthermore, when coexist of both, a red-to-green signal shift occurred. It is these superior properties that have led to the successful application of **BPC** in subcellular organelle and living mice to real-time visualizing the biological process of Cys metabolizing SO_2. We expect that probe **BPC** can be a dynamic monitoring tool with medical value in preventing related diseases caused by metabolic disorders of Cys using fluorescence technology.

We thank the National Natural Science Foundation of China (No. 21775096), Shanxi Province"1331 project" key innovation team construction plan cultivation team (2018-CT-1), 2018 Xiangyuan County Solid Waste Comprehensive Utilization Science and Technology Project (2018XYSDJS-05), the Shanxi Province Foundation for Selected (No. 2019), Innovative Talents of Higher Education Institutions of Shanxi, Scientific and Technological Innovation Programs of Higher Education Institutions in Shanxi (2019L0031), Key R&D Program of Shanxi Province (201903D421069), the Shanxi Province Science Foundation (No. 201901D111015), China Institute for Radiation Production and Scientific Instrument Center of Shanxi University (201512).

Conflicts of interest

View Article Online
DOI: 10.1039/D0CC04839A

There are no conflicts to declare.

Notes and references

1. (a) K. G. Reddie and K. S. Carroll, *Curr. Opin. Chem. Biol.*, 2008, **12**, 746-754. (b) E. Weerapana, C. Wang, G. M. Simon, F. Richter, S. Khare, M. B. D. Dillon, D. A. Bachovchin, K. Mowen, D. Baker and B. F. Cravatt, *Nature,* 2010, **468**, 790-795.
2. (a) M. T. Heafield, S. Fearn, G. B. Steventon, R. H. Waring, A. C. Williams and S. G. Sturman, *Neurosci. Lett.*, 1990, **110**, 216-220. (b) L. Y.Niu, Y. S. Guan, Y. Z. Chen, L. Z. Wu, C. H. Tung and Q. Z. Yang, *Chem. Commun.*, 2013, **49**, 1294-1296
3. (a) Y. Yue, F. Huo, P. Ning, Y. Zhang, J. Chao, X. Meng and C. Yin, *J. Am. Chem. Soc.,* 2017, **139**, 3181-3185. (b) J. Liu, M. X. Liu, H. X. Zhang, X. H. Wei, J. J. Wang, M. Xian and W. Guo, *Chem. Sci.*, 2019, **10**, 10065-10071.
4. (a) T. Ubuka, J. Ohta, R. Akagi, Y. Hosaki, Y. Ishimoto, S. Kiguchi, T. Ikeda and K. Ishino, *Amino Acids,* 1992, **3**, 243-252. (b) L. M. Luo, S. Chen, H. F. Jin, C. S. Tang and J. B. Du, *Biochem. Biophys. Res. Commun.*, 2011, **415**, 61-67. (c) D. P. Li, Z. Y. Wang, X. J. Cao, J. Cui, X. Wang, H. Z. Cui, J. Y. Miao and B. X. Zhao, *Chem. Commun.*, **2016**, *52*, 2760-2763
5. (a) G. Chen, W. Zhou, C. Y. Zhao, Y. X. Liu, T. Chen, Y. L. Li and Tang, B. *Anal. Chem.*, 2018, **90**, 12442-12448. (b) W. Zhang, F, Huo and C. Yin, *Org. Lett.*, 2019, **21**, 5277-5280.
6. P. Gao, W. Pan, N. Li and B. Tang, *Chem. Sci.*, 2019, **10**, 6035-6071.
7. (a) M. M. Xing, K. N. Wang, X. W. Wu, S. Y. Ma, D. X. Cao, R. F. Guan and Z. Q. Liu, *Chem. Commun.,* 2019, **55**, 14980-14983; (b) D. X. Cao, Z. Q. Liu, P. Verwilst, S. Koo, P. Jangjili, J. S. Kim and W. Y. Lin, *Chem. Rev.,* 2019, **119**, 10403-10519; (c) L. Y. Niu, Y. S. Guan, Y. Z. Chen, L. Z. Wu, C. H. Tung and Q. Z. Yang, *J. Am. Chem. Soc.,* 2012, **134**, 18928-18931.
8. (a) B.J. Wang, R. J. Liu, J. G. Fang, Y. W. Wang and Y. Peng, *Chem. Commun., 2019*, **55**, 11762-11765 (b) L. J. Tang, P. He, X. M. Yan, J. Z. Sun, K. L. Zhong, S. H. Hou and Y. J. Bian, *Sens. Actuators B: Chem.,* 2017, **247**, 421-427; (c) B. Y. Xu, H. B. Zhou, Q. S. Mei, W. Tang, Y. L. Sun, M. P. Gao, C. L. Zhang, S. S. Deng and Y. Zhang, *Anal. Chem.,* 2018, **90**, 2686-2691.
9. J. W. Chen, X. Q. Jiang, S. L. Carroll, J. Huang and J. Wang, *Org. Lett.,* 2015, **17**, 5978-5981.
10. Y. Y. Ma, W. J. Gao, L. L. Zhu, Y. P. Zhao and W. Y. Lin, *Chem. Commun.*, 2019, **55**, 11263-11266.
11. K. E. Sapsford, L. Berti and I. L. Medintz, *Angew. Chem., Int. Ed.* 2006, **45**, 4562–4588.
12. (a) H. L. Zhang, P. F. Xu, X.T. Zhang, X. Z. Cao, W. X. Han, M. H. Liu, X. H. Liu and W. B. Zang, *Chin. Chem. Lett.,* 2020, **31**, 1083-1086. (b) Y. Yan, X. D. Zhang, X. F. Zhang, N. Li, H. Z. Man, L. C. Chen and Y. Xiao, *Chin. Chem. Lett.,* 2020, **31**, 1091-1094.
13. M. H. Stipanuk, J. J. E. Dominy, J.-I. Lee and R. M. Coloso, *J. Nutr.*, 2006, **136**, 1652S-1659S.

View Article Online
DOI: 10.1039/D0CC04839A

Abstract Graphic